

## Charge ratio of muons from atmospheric neutrinos

T.K. Gaisser & Todor Stanev  
 Bartol Research Institute, University of Delaware  
 Newark, DE 19716 USA

We calculate the intensities and angular distributions of positive and negative muons produced by atmospheric neutrinos. We comment on some sources of uncertainty in the charge ratio. We also draw attention to a potentially interesting signature of neutrino oscillations in the muon charge ratio, and we discuss the prospects for its observation (which are not quite within the reach of currently planned magnetized detectors).

The MINOS detector [1] under construction in the Soudan Mine for study of neutrino oscillations with a neutrino beam from Fermilab will be able to measure the momentum and charge of muons in the energy range from just below one GeV to about 70 GeV/c. [2] In addition to its use as the far detector for accelerator neutrinos, MINOS is sufficiently large to detect a significant number of atmospheric neutrinos. Muons entering from outside the detector as well as muons originating from vertices inside the detector will occur. These events will provide a useful calibration beam for the detector.

The detector, which is now under construction at Soudan, has already detected atmospheric muons and neutrinos. After completion, MINOS will continue to collect cosmic-ray data for some time before the accelerator neutrino beam turns on and afterwards as well. Because the atmospheric neutrino beam has comparable fluxes of neutrinos and anti-neutrinos, it will be possible [3,2] to search for any sign of differences in oscillation properties of  $\nu_\mu$  and  $\bar{\nu}_\mu$ . Such differences could arise in theories in which there is intrinsic violation of CPT [4]. They could also arise from matter effects, for example with mixing of three active neutrino flavors if  $\sin^2\theta_{12}$  is large enough [5] or with non-maximal  $\nu_\mu \leftrightarrow \nu_s$  mixing. [6]

The purpose of this letter is to calculate the rates of atmospheric neutrino interactions in a detector like MINOS as a function of direction and energy separately for neutrinos and anti-

neutrinos. We briefly discuss some sources of systematic uncertainty, and we note a potentially interesting effect of oscillations as reflected in the charge ratio of atmospheric muons.

To illustrate the basic result, we start with the atmospheric neutrino spectrum of Ref. [7]. We integrate the spectra of atmospheric neutrinos folded with  $d\sigma/dy$  to obtain the rate of events with contained vertices. To obtain the rates of external muons, the convolution also includes the muon range. [8,9] For simplicity we use the GRV94 structure functions [10] to obtain the spectra of neutrino-induced  $\mu^+$  and  $\mu^-$ . (We have checked that the results for the limited range of  $x$  and  $Q^2$  relevant here are essentially the same as those obtained with more complicated structure functions.) In Table 1 we show expected event rates as a function of muon energy with and without oscillations, separately for contained vertices and for external upward-moving neutrino-induced muons. Full mixing with  $\Delta m^2 = 2.5 \times 10^{-3} \text{ eV}^2$  [11] was assumed for the oscillation case. Contained vertices are shown integrated over all directions; neutrino-induced muons are summed over the upward  $2\pi$  steradian.

The first point to note is that the charge ratio for neutrino-induced muons is reversed relative to that for atmospheric muons. There are more negative than positive neutrino-induced muons ( $\mu^+/\mu^- \lesssim 1/2$ ), whereas for muons produced in the atmosphere,  $\mu^+/\mu^- \approx 1.25$  [12] This is a consequence of the ratio of cross sections,  $\sigma_\nu/\sigma_{\bar{\nu}} > 1$ , and the fact that  $\nu_\mu \rightarrow \mu^-$  while  $\bar{\nu}_\mu \rightarrow \mu^+$ . In

Table 1

Event rates for vertex contained and upward external neutrino induced muons at the location of MINOS for the epoch of solar minimum in four energy intervals, with and without oscillations. The oscillation parameters used are  $\sin^2 2\theta = 1$  and  $\Delta m^2 = 0.0025 \text{ eV}^2$ . The units for vertex contained events are  $10^{-16} g^{-1}.s^{-1}$  and for external upward going muons are  $10^{-13} cm^{-2}.s^{-1}$

E, GeV	no oscillations		$\Delta m^2 = 0.0025 \text{ eV}^2$	
	$\mu^-$	$\mu^+$	$\mu^-$	$\mu^+$
	contained vertex			
1 - 5	6.88	3.27	5.14	2.45
5 - 10	0.86	0.41	0.66	0.31
10 - 20	0.48	0.24	0.38	0.18
>20	0.49	0.23	0.46	0.21
	external upward going			
1 - 5	3.57	1.71	2.01	0.94
5 - 10	1.58	0.75	1.05	0.48
10 - 20	1.55	0.72	1.21	0.54
> 20	5.38	2.19	5.20	2.10

addition, the ratio  $\nu_\mu/\bar{\nu}_\mu$  increases slowly above its low energy value of unity, first as muon-decay becomes unimportant and at higher energy because of the increasing importance of the channel  $p \rightarrow \Lambda K^+ \rightarrow \nu_\mu \mu^+$ .

Secondly, the energy spectrum of the external muons is significantly harder than for the contained vertices. This is a consequence of the increase of the muon range with energy. A much higher range of neutrino energies contributes to the external events than to the events with interaction vertex inside the detector. For  $E_\nu > 100 \text{ GeV}$  kaons become the dominant source of neutrinos, with a big contribution from the process  $p \rightarrow \Lambda K^+ \rightarrow \nu_\mu$ . As a result, the charge asymmetry is somewhat larger for external events than for contained vertices.

It is also interesting to look at the angular dependence of neutrino-induced muons with and without oscillations. Fig. 1 shows the zenith angle dependence of the neutrinos that produce muons with contained vertices and upward going neutrino-induced muons originating outside the

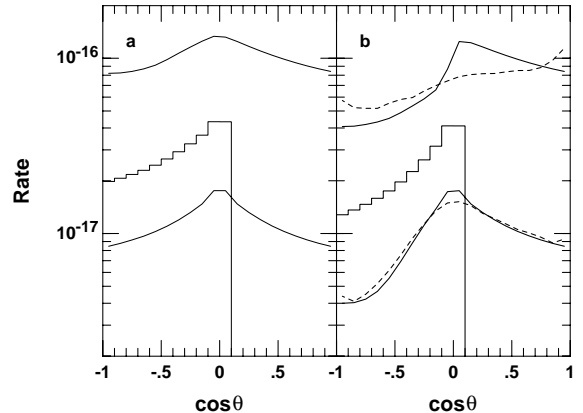


Figure 1. a) Zenith angle dependence of the neutrinos generating vertex contained muons of energy above 1 GeV (upper line) and 10 GeV (lower line) and of upward going external muons (histogram) in the absence of oscillations. The units for vertex contained events are  $(g.s.sr)^{-1}$  and for external upward going muons are  $(cm^2.s.sr)^{-1}$ . The flux of upward going muons is divided by  $10^4$ . Note that the upward going muons are plotted up to  $\cos\theta = 0.1$ ; b) Same in the presence of oscillations with  $\sin^2 2\theta = 1$  and  $\Delta m^2 = 0.0025$ . The dashed lines show the zenith angle dependence of the muons.

detector. The strongest effect of oscillations is on the contained vertex events above 1 GeV.

The symmetric shape of the no oscillation case is replaced by an asymmetric distribution with a deficit due to oscillations for upward muons from neutrinos with pathlengths comparable to the radius of the Earth. This effect is in reality obscured by the large angle between the neutrino and muon direction at low energy as shown by the dashed lines in Fig. 1b. The effect of the oscillations is also obvious in the higher energy ( $E > 10 \text{ GeV}$ ) sample. The rate of vertically upgoing contained vertex muons is decreased by a factor of  $\sim 2$ . The muon-neutrino angle in this case is significantly smaller and does not affect much the oscillation features. The smallest effect is in the case of external events. On one hand, the contri-

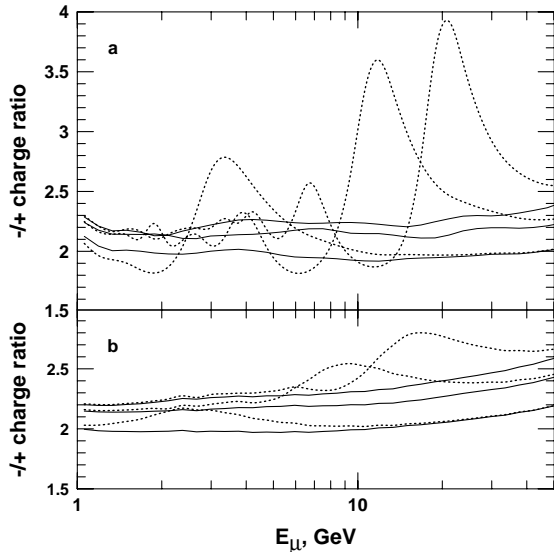


Figure 2. Charge ratio of neutrino-induced muons a) for events with contained vertices; b) for external muons. Solid lines are with no oscillations and dotted lines with oscillations for three bins of zenith angle centered on  $\cos\theta = -0.95, -0.55$  and  $-0.15$ . Near vertical is highest solid line (rightmost dotted peak).

bution of high energy, non-oscillating neutrinos is the largest and on the other the downgoing external muon rate is dominated by atmospheric muons, so most of the downward hemisphere is not available as a probe of neutrino oscillations with external events. The muon–neutrino angle for this sample is negligible. The background of atmospheric muons is low enough at the depth of Soudan so that neutrino-induced, external muons can be measured up to  $\cos\theta \approx 0.1$ , about  $6^\circ$  above the horizon. Integrated over all upward-going external events the, oscillations decrease the rate by 22%, which is comparable to the uncertainty in the expected flux. [13] Instead, the effect of oscillations is visible as a distortion of the angular distribution, as observed at MACRO [14] and Super-K. [15]

We assume here that neutrinos and anti-

neutrinos have identical oscillations properties. Because of the properties of the differential charged current cross sections of neutrinos, however, the relation between  $E_\nu$  and  $E_\mu$  is different for  $\nu_\mu$  and  $\bar{\nu}_\mu$ . As a consequence, when the muon charge ratio is plotted as a function of muon energy for a given angular bin (corresponding to a given pathlength) oscillation features appear in the ratio because the oscillation minima show up at different energies for  $\mu^+$  and  $\mu^-$ . Figure 2 illustrates this for contained vertices (a) and for external muons (b). The ratios are shown for three bins of  $\cos\theta$  going from nearly vertical ( $-1 < \cos\theta < -0.9$ ) to nearly horizontal ( $-0.2 < \cos\theta < -0.1$ ). The solid lines show the charge ratios in the absence of oscillations. The baseline charge ratio increases slightly at high energy and is larger near the vertical because of the increased importance of kaon decay relative to pion decay.

Calculation of external events involves an integral over all contributing neutrino energies taking account of the increase of muon range with energy. The growth of the charge ratio with muon energy is stronger than for contained vertices because of the contribution of higher energy neutrinos. In the oscillation case the variations are smaller than for contained vertex events and do not show the secondary sinusoidal features. For the external events, the peaks are wider and shallower than for contained vertices because of the contribution of a broader range of neutrino energies.

For more insight into the origin of this behavior, we show in Fig. 3 the charge ratio with and without oscillations for the vertically upward bin of zenith angle, for which the pathlength  $L \sim 10^4$  km. The lower panel shows the corresponding survival probability, which is assumed identical for neutrinos and antineutrinos. An approximate, quantitative understanding of the features can be obtained by considering the leading term in the differential neutrino charged current cross sections. For neutrinos

$$\frac{d\sigma(E_\nu)}{dz^-} \approx \sigma_0 \times E_\nu/GeV \quad (1)$$

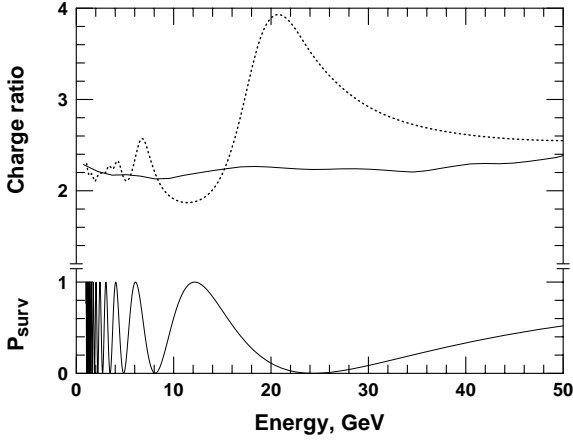


Figure 3. Upper part shows the variation of the  $\mu^-/\mu^+$  charge ratio of almost vertical ( $\cos\theta = -0.95$ ), vertex contained upward-going neutrino-induced muons as a function of muon energy for no oscillations (solid) and oscillations (dotted line). The lower part shows the neutrino survival probability for the same angular bin.

and

$$\frac{d\sigma(E_{\bar{\nu}})}{dz^+} \approx \sigma_0 \times (z^+)^2 \times E_{\bar{\nu}}/GeV \quad (2)$$

for antineutrinos. Here  $0 \leq z = E_{\mu^-}/E_{\nu} \leq 1$  and  $\sigma_0 \approx 0.8 \times 10^{-38} \text{cm}^2$ . Using the approximation 1 we can estimate the relation for neutrinos by evaluating the average  $E_{\nu}$  for the distribution

$$\phi(E_{\nu}) \frac{d\sigma(E_{\nu})}{dE_{\mu^-}}. \quad (3)$$

Here

$$\phi(E_{\nu}) \propto E_{\nu}^{-(\gamma+1)} \quad (4)$$

is a power-law approximation for the differential spectrum of neutrinos. Then

$$\langle E_{\nu} \rangle \approx \frac{\gamma}{\gamma-1} E_{\mu^-}. \quad (5)$$

The corresponding result for antineutrinos is

$$\langle E_{\bar{\nu}} \rangle \approx \frac{\gamma+2}{\gamma+1} E_{\mu^+}. \quad (6)$$

With  $\gamma \approx 2$  in the relevant energy range [7], we have  $E_{\bar{\nu}}/E_{\mu^+} \approx 4/3$  and  $E_{\nu}/E_{\mu^-} \approx 2$ . Thus the first oscillation minimum at  $\approx 24$  GeV should be reflected at  $\approx 18$  GeV in  $\bar{\nu}_{\mu}$  and  $\mu^+$  as an increase in the  $\mu^-/\mu^+$  ratio and at  $\approx 12$  GeV in the opposite channel, reflected as the minimum in the  $\mu^-/\mu^+$  ratio below 12 GeV. The slight deviations from these numbers in Fig. 3 reflect the breadth and asymmetry of the oscillation features folded with the neutrino spectrum.

Unfortunately, the MINOS detector is not large enough to see the oscillation effect in the charge ratio well, if at all. For example, we estimate that there will be only some 12  $\mu^-$  and 5  $\mu^+$  events with energy between 10 and 30 GeV in 25 kt-yr in the angular region  $-1 < \cos\theta < -0.5$ , where the charge ratio is high (see Fig. 2). Our estimates are based on the angular distribution of the interacting neutrinos and do not account for the experimental efficiency.

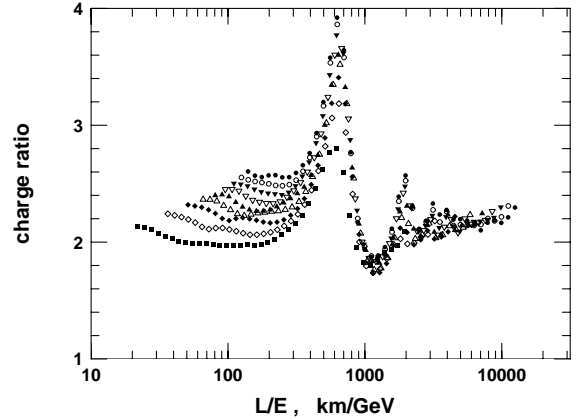


Figure 4. Charge ratio of  $\mu^-/\mu^+$  for upward going contained vertex neutrino induced muons as a function of  $L/E$  for different zenith angles. Different symbols show events in  $\cos\theta$  bins of  $-0.15, -0.25, -0.35, \dots, -0.95$ . The horizontal case is not plotted because of the very strong change of the oscillation length which requires a much more exact calculation.

The best way to use all the data is to bin every event by  $L/E$ . Fig. 4 shows the charge ratio in upward going contained vertex events for the standard oscillation parameters as a function of  $L/E$  for nine different  $\cos\theta$  bins. The horizontal bin is not included because the fast change of the oscillation length there requires a much more exact calculation. One can easily identify the peaks and valleys in the charge ratio that follow the oscillation structure of the atmospheric neutrino flux. The main feature is at  $L/E$  of  $\sim 600$ , where the charge ratio can grow to almost twice its baseline value of  $\mu^-/\mu^+ \approx 2$ . The valley is at  $L/E$  of  $\sim 1200$ . One can subdivide the  $L/E$  range in two parts with different charge ratios, 2.36 in the  $L/E$  from 300 to 900 and 1.84 from 900 to 1500. The expected number of muons for 25 kT.yr are 26.7  $\mu^-$  & 11.3  $\mu^+$  and 15.5 & 8.4 respectively, still very small statistics.

One should also note that Fig. 4 shows the neutrino pathlength  $L$  which is not experimentally measured. For some of these events, where the sinusoidal variation happens at energies below 10 GeV, the angular smearing of the neutrino-muon angle will seriously obscure the effect when plotted as  $L_\mu/E_\mu$ .

It is interesting to ask if one could distinguish oscillations from neutrino decay with an observation of the muon charge ratios. The  $L/E < 1500$  part of Fig. 4 would not change for a decay scenario that fits the muon disappearance observations. At higher  $L/E$  values the charge ratio behavior would be much smoother without the secondary and tertiary peaks at  $L/E$  of about 2000 and 3000. The increase of the charge ratio at these positions are however small and even more difficult to detect.

The reliable detection of the variation of the muon charge ratio would require a much bigger detector. The MONOLITH [16] detector with mass of 30 kT was proposed for the Gran Sasso Laboratory. If this detector had been built and were operated for five years it would be able to measure the effect at the  $3\sigma$  level.

The MINOS detector will be able to measure the total neutrino energy but assume that the muon and neutrino directions coincide. The difference between the neutrino and muon energy

spectra as a function of  $L$ , as well as the charge ratios, could provide additional observable parameters for the more exact derivation of the oscillation parameters.

The exact manifestation of the effect however has systematic uncertainties related to the uncertainties of the atmospheric flux. These arise from the limited knowledge of the primary cosmic ray spectrum and the production of pions and kaons. The overall uncertainty for  $E_\nu \sim 10$  GeV is estimated in Ref. [17] as  $\pm 25\%$ .

The uncertainty in the ratio  $\nu_\mu/\bar{\nu}_\mu$  should be significantly less than the uncertainty in the magnitude of the flux because the normalization of the primary cosmic ray spectrum cancels. The largest remaining source of uncertainty in the ratio is from production of charged pions and kaons, especially in the forward fragmentation region, as reflected by the spectrum weighted moments,  $Z_{p\pi^+}$ ,  $Z_{p\pi^-}$ ,  $Z_{pK^+}$  and  $Z_{pK^-}$ . For pions and especially for kaons, the positive channel dominates, and kaons become relatively more important at high energy.

We can estimate the uncertainty in the  $\nu_\mu/\bar{\nu}_\mu$  ratio by combining in quadrature the estimates in Ref. [7] of uncertainty in the flux of  $\nu_\mu + \bar{\nu}_\mu$  from each of the four channels independently. This leads to an estimate of  $\pm 8\%$  below 10 GeV and  $\pm 9\%$  for  $10 < E_\nu < 100$  GeV. Analysis of data from forthcoming hadron production experiments with CERN [18,19] and Fermilab [20] should lead to a reduction of this estimate.

The effect we described above should also be detectable in a slightly different form in the long baseline oscillation experiment with the NuMI neutrino beam. The experimental statistics would be fully sufficient and the exact manifestation would strongly depend on the beam energy spectrum, purity, and composition. All of these three parameters are currently still at the design stage.

**Acknowledgments.** We are grateful for helpful discussions with Doug Michael and Teresa Montaruli. This work is supported in part by the U.S. Dept. of Energy under Grant No. DE-FG02-91ER40626.

## REFERENCES

1. S. Wojcicki, Nucl. Phys. B91 (Proc. Suppl.) (2001) 216.
2. D. Michael, to appear in Proc. Neutrino2002.
3. The Minos Collaboration, Proposal for a Cosmic Ray Veto Shield for the MINOS Far Detector (2002).
4. See e.g. G. Barenboim et al., Phys. Lett. B537 (2002), 227.
5. J. Bernabéu & S. Paolmares-Ruiz, hep-ph/0112002 and hep-ph/0201090.
6. F. Ronga & F. Terranova, Monolith-003/00.
7. V. Agrawal, T.K. Gaisser, Paolo Lipari & Todor Stanev, Phys. Rev. D53 (1996) 1314.
8. T.K. Gaisser & T. Stanev, Phys. Rev. D30 (1984) 985.
9. T.K. Gaisser & T. Stanev, Phys. Rev. D31 (1985) 2770.
10. M. Gluck, E. Reya & A. Vogt, Z. Phys. C67 (1995) 433.
11. C. Mauger, Super-Kamiokande Collaboration, Proc. 31st Int. Conf. on High Energy Physics (Amsterdam) July, 2002.
12. M. Motoki et al. (The BESS Collaboration) *astro-ph/0205344*.
13. T.K. Gaisser, M. Honda, Paolo Lipari & Todor Stanev, Proc. 27th Int. Cosmic Ray Conf. (Hamburg, 2001) 1643.
14. M. Ambrosio *et al.*, Phys. Lett. B517 (2001) 59.
15. Y. Fukuda *et al.*, Phys. Rev. Lett. 82 (1999) 2644.
16. For the MONOLITH proposal and related work, see <http://castore.mib.infn.it/monolith/>.
17. T.K. Gaisser & M. Honda, Ann. Revs. Nucl. Part. Sci. 52 (2002) 153.
18. G. Barr, Proc. 27th Int. Cosmic Ray Conf. (Hamburg, 2001)
19. M.G. Catanesi et al., Proposal for hadron production measurements using the NA49 detector for use in long baseline and atmospheric neutrino flux calculations, EXP CERN-NA-049 (2001)
20. MIPP (Main Injector Particle Production experiment) Proposal FNAL-E-0907.